Clustered Negative Charges on the Lipid Membrane Surface Induce β-Sheet Formation of Prion Protein Fragment 106−126

Takashi Miura, Mayumi Yoda, Naoyuki Takaku, Takanori Hirose, and Hideo Takeuchi*

Graduate School of Pharmaceutical Sciences, Tohoku University, Aobayama, Sendai 980-8578, Japan

Received May 18, 2007; Revised Manuscript Received August 10, 2007

ABSTRACT: The conformational conversion of prion protein (PrP) from an α-helix-rich normal cellular isoform (PrP^C) to a β-sheet-rich pathogenic isoform (PrP^{Sc}) is a key event in the development of prion diseases, and it takes place in caveolae, cavelike invaginations of the plasma membrane. A peptide homologous to residues 106−126 of human PrP (PrP106−126) is known to share several properties with PrP^{Sc}, e.g., the capability to form a β-sheet and toxicity against PrP^C-expressing cells. PrP106−126 is thus expected to represent a segment of PrP that is involved in the formation of PrP^{Sc}. We have examined the effect of lipid membranes containing negatively charged ganglioside, an important component of caveolae, on the secondary structure of PrP106−126 by circular dichroism. The peptide forms an α-helical or a β-sheet structure on the ganglioside-containing membranes. The β-sheet content increases with an increase of the peptide:lipid ratio, indicating that the β-sheet formation is linked with self-association of the positively charged peptide on the negatively charged membrane surface. Analogous β-sheet formation is also induced by membranes composed of negatively charged and neutral glycerophospholipids with high and low melting temperatures, respectively, in which lateral phase separation and clustering of negatively charged lipids occur as shown by Raman spectroscopy. Since ganglioside-containing membranes also exhibit lateral phase separation, clustered negative charges are concluded to be responsible for the β-sheet formation of PrP106−126. In caveolae, clustered ganglioside molecules are likely to interact with the residue 106−126 region of PrP^C to promote the PrP^C-to-PrP^{Sc} conversion.

Prion protein (PrP)[1] is a glycosylphosphatidylinositol (GPI)-anchored membrane protein predominantly expressed in neuronal tissue (*1*). Mature mammalian PrP after post-translational modifications spans residues 23−231 of the 253-amino acid sequence coded by a single gene (*2*). NMR studies have revealed that the C-terminal half (residues 121−231) of PrP has a compact globular structure consisting of three α-helices and two short antiparallel β-strands, whereas the N-terminal half of the protein is structurally disordered (*3*−*7*). Conformational transition of PrP from the α-helix-rich normal cellular isoform (PrP^C) to a β-sheet-rich pathogenic isoform (PrP^{Sc}) is considered to be responsible for prion diseases (*8*), which are fatal transmissible neurodegenerative disorders of humans and animals (*9*−*11*). PrP^{Sc} is resistant to protease and shows a strong tendency toward polymerization into insoluble fibrils that disrupt neuronal function (*10*, *11*). Despite extensive investigations, the mechanism of the PrP^C-to-PrP^{Sc} conversion has not yet been clarified.

Studies on the localization of PrP in neuroblastoma cells have revealed that both PrP^C and PrP^{Sc} exist in caveolae (*12*, *13*). Caveolae are cavelike invaginations of the cell surface enriched with a structural protein (caveolin), cholesterol, and sphingolipids (*14*−*17*). The existence of PrP^C in caveolae is not unusual because GPI-anchored proteins are frequently found in caveolae (*18*). The additional presence of PrP^{Sc}, on the other hand, strongly suggests that the PrP^C-to-PrP^{Sc} conversion takes place in caveolae. The involvement of caveolae in the PrP^C-to-PrP^{Sc} conversion is consistent with the observation that the PrP^{Sc} formation was diminished when caveolae were disrupted by cholesterol depletion (*19*, *20*) or when the GPI anchoring was inhibited by deletion or replacement of the C-terminal anchor region of PrP^C (*19*, *21*). Caveolae provide a place not only for the GPI anchoring of PrP^C but also for the conversion from PrP^C to PrP^{Sc}.

Since caveolae are membrane microdomains of characteristic compositions, it is possible that interaction of PrP^C with a caveolar component plays a role in the PrP^C-to-PrP^{Sc} conversion. Studies using model lipid membranes have shown that PrP^C binds to membranes containing negatively charged glycerophospholipids and becomes richer in β-sheet structure (*22*−*24*). The propensity of PrP to undergo a conformational transition through interaction with negatively charged membranes may be relevant to the molecular mechanism of the PrP^C-to-PrP^{Sc} conversion in caveolae, because caveolae contain significant amounts of negatively charged ganglioside, a class of sphingolipid bearing one or more anionic sialic acid residues in the head group (*16*).

* To whom correspondence should be addressed. Phone/fax: +81-22-795-6855. E-mail: takeuchi@mail.tains.tohoku.ac.jp.

[1] Abbreviations: MW, molecular weight; asialo-GM1, galactosyl-(*N*-acetylgalactosaminyl)galactosylglucosylceramide; BGS, bovine brain-extracted ganglioside; BPC, bovine brain-extracted L-α-phosphatidylcholine; BPS, porcine brain-extracted L-α-phosphatidylserine; DMPS, 1,2-dimyristoyl-*sn*-glycero-3-phospho-L-serine; GPI, glycosylphosphatidylinositol; GM1, galactosyl(*N*-acetylgalactosaminyl)(*N*-acetylneuraminyl)galactosylglucosylceramide; POPC, 1-palmitoyl-2-oleoyl-*sn*-glycero-3-phosphocholine; POPS, 1-palmitoyl-2-oleoyl-*sn*-glycero-3-phospho-L-serine; PrP, prion protein; PrP106−126, peptide homologous to residues 106−126 of human prion protein; PrP^C, normal cellular prion protein; PrP^{Sc}, pathogenic prion protein; T_m, melting temperature.

10.1021/bi700939j CCC: $37.00
Published on Web 09/22/2007

Immunostaining confocal microscopy has shown that PrP^C molecules are localized in the membrane microdomains enriched with gangliosides (*25*), suggesting a specific interaction between PrP^C and ganglioside.

A peptide representing residues 106−126 of human PrP (PrP106−126) has been found to exhibit toxicity against PrP^C-expressing cells as PrP^{Sc} does (*26*, *27*). PrP106−126 also shows a conformational flexibility to form a β-sheet, a strong tendency to aggregate into fibrils, and a partial resistance to protease digestion (*28*−*30*). These properties of PrP106−126 are analogous to those of the full-length protein PrP, suggesting that PrP106−126 may represent a segment of PrP that is involved in the conformational transition from PrP^C to PrP^{Sc} in caveolae. However, no systematic studies have been reported on the interaction of PrP106−126 with lipid membranes, in particular those containing ganglioside.

In this study, we have investigated the interaction of PrP106−126 with lipid membranes containing ganglioside or other negatively charged lipids by using circular dichroism (CD) and Raman spectroscopy. The results show that positively charged PrP106−126 binds to negatively charged membranes and forms an α-helical or a β-sheet structure. The lipid-induced secondary structure formation takes place under solution conditions where the peptide does not spontaneously fold into an α-helix or a β-sheet. The β-sheet formation is specifically promoted when PrP106−126 is concentrated on membranes containing clusters of negatively charged lipids. Ganglioside molecules tend to self-aggregate laterally in membranes to produce clusters of surface negative charges (*31*−*36*). It is therefore likely that clustered ganglioside molecules in caveolae play a key role in the PrP^C-to-PrP^{Sc} conversion through interaction with the residue 106−126 region of PrP.

MATERIALS AND METHODS

Preparation of the Peptide. A 21-mer peptide homologous to residues 106−126 of human PrP (PrP106−126, Lys-Thr-Asn-Met-Lys-His-Met-Ala-Gly-Ala-Ala-Ala-Ala-Gly-Ala-Val-Val-Gly-Gly-Leu-Gly) was synthesized on an automated peptide synthesizer (Applied Biosystems model 431A) from amino acid derivatives protected by the 9-fluorenylmethoxycarbonyl group. The N and C termini of the peptide were capped with acetyl and amide groups, respectively, to remove charges on the termini and to mimic the corresponding region of the protein PrP. The crude peptide was cleaved from the resin and purified by HPLC on a reversed-phase column (Cosmosil $5C_{18}$-AR, Nacalai Tesque) using a 20−40% linear gradient of acetonitrile in 0.1% (v/v) trifluoroacetic acid. The purified peptide was identified by mass spectrometry (*m*/*z* 1954). Lyophilized powder of the peptide was dissolved in 100 mM hydrochloric acid and again lyophilized to remove residual trifluoroacetic acid. The final product was obtained as the hydrochloride salt (powder) and kept in a freezer. The peptide concentration was measured by using the intensity of a *N*-deuterated histidine Raman band at 1408 cm^{-1} against a water (D_2O) Raman band at 1204 cm^{-1} in acidic D_2O solution. The histidine Raman band intensity was proportional to the weight of peptide dissolved in D_2O up to 5 mM, ensuring that the peptide was completely dissolved at the concentrations (25 μM or below) employed in the present peptide−lipid interaction experiments. Throughout the sample preparation, the peptide solution was controlled not to be highly concentrated at alkaline pH to avoid self-aggregation of the peptide around its isoelectric point (pI ≈ 10).

Lipids. The gangliosides used to prepare liposomes are GM1, asialo-GM1, and bovine brain-extracted ganglioside (BGS). GM1 contains one sialic acid (*N*-acetylneuraminic acid) residue per molecule with a molecular weight (MW) of about 1540 estimated from the most abundant (70%) molecular species having one each of stearic (C18:0) and oleic (C18:1) acyl chains. Asialo-GM1 (average MW ≈ 1250) is a GM1 analogue devoid of the sialic acid residue, while BGS is a mixture of GM1, GD1a, GT1b, etc. containing about 20% (w/w) sialic acid. [The ganglioside nomenclature follows that of Svennerholm (*37*).] The other natural lipids used were bovine brain-extracted L-α-phosphatidylcholine (BPC; number average MW 770) and porcine brain-extracted L-α-phosphatidylserine (BPS; number average MW 810). The following synthetic lipids were also used: 1-palmitoyl-2-oleoyl-*sn*-glycero-3-phosphocholine (POPC), 1-palmitoyl-2-oleoyl-*sn*-glycero-3-phospho-L-serine (POPS), and 1,2-dimyristoyl-*sn*-glycero-3-phospho-L-serine (DMPS). BGS, GM1, asialo-GM1, and BPC were purchased from Sigma-Aldrich. The other lipids were obtained from Avanti Polar Lipids. All the lipids were used as received.

Preparation of Liposomes. Small unilamellar liposomes were prepared in the following way: Lipids were dissolved in a 1:1 (v/v) chloroform/methanol mixture, and the solution was spread as a thin layer onto the wall of a round-bottom flask by removing the solvent with a rotary evaporator. Complete removal of the solvent was done by drying under vacuum overnight. Deionized water was then added to the flask, and the lipid film was hydrated under vortexing for 10 min. The suspension containing multilamellar vesicles was sonicated using an ultrasonic generator with a tip probe (Nihonseiki, US-50) until the suspension became transparent (for about 5 min). Titanium particles from the tip probe were removed by centrifugation. The supernatant was extruded 21 times through a polycarbonate filter of 50 nm pore size (Liposofast) to obtain a suspension of small unilamellar liposomes. Liposomes thus prepared are known to be reasonably homogeneous with an average diameter close to the pore size of the filter (*38*). The liposome suspensions were used within a day of preparation.

CD Spectra of PrP106−126. Lyophilized powder of PrP106−126 was dissolved in liposome suspensions of defined lipid concentrations and volumes. In examining the effect of the peptide concentration on the CD spectrum, a small amount of PrP106−126 powder was successively added to a peptide−liposome mixture suspension. The pH of the suspension (200 μL) was adjusted to 7.4 by carefully adding an aliquot (∼1 μL) of concentrated (175 mM) aqueous NaOH. (The increase in the salt concentration by this pH adjustment was estimated to be less than 1 mM.) The samples were equilibrated for 1 h at room temperature before spectral measurement. CD spectra were recorded on a Jasco J-820 spectropolarimeter using a quartz cell of 0.5 mm path length and averaged over four scans for each sample. The background signal due to the cell and lipid was recorded separately and subtracted from the spectra of peptide−liposome suspensions. The photomultiplier electrical voltage of the spectropolarimeter, an indicator of the sample

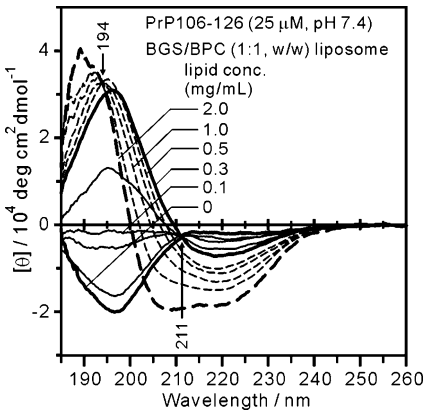

FIGURE 1: Lipid concentration dependence of the CD spectrum of PrP106−126 (25 μM, pH 7.4). CD spectra were recorded in the presence of various concentrations of liposomes prepared from a 1:1 (w/w) mixture of BGS and BPC. The spectra at total lipid concentrations of 0, 0.025, 0.075, 0.1, 0.2, and 0.3 mg/mL are drawn with solid lines and those at 0.5, 0.75, 1.0, 1.5, and 2.0 mg/mL with broken lines. The spectra mainly due to irregular, β-sheet, and α-helical structures are emphasized with bold lines. The ordinate shows the molar ellipticity per residue. Isodichroic points at 194 and 211 nm are indicated with arrows.

opacity, did not differ largely between peptide-free and peptide-bound liposomes, indicating that no disruption nor aggregation of liposomes was caused by the addition of the peptide. The pH values measured before and after the CD spectral acquisition were substantially identical.

Raman Spectra of Liposomes. Raman spectroscopy was utilized to detect lateral phase separation in DMPS/POPC and POPS/POPC mixture membranes. Liposomes prepared from an equimolar mixture (2.5 mM each) of DMPS/POPC or POPS/POPC at pH 7.4 were sealed in a glass capillary tube and excited with the 514.5 nm line of a Coherent Innova 70 Ar^+ laser. The sample temperature was regulated at 10−60 °C with a constant-temperature circulator. Raman scattered light was collected with a camera lens and dispersed on a Jasco NR-1800 triple spectrometer equipped with a liquid-nitrogen-cooled CCD detector.

RESULTS

Secondary Structure of PrP106−126 and Its Change upon Binding to Ganglioside-Containing Liposomes. The CD spectrum of PrP106−126 in lipid-free aqueous solution (25 μM, pH 7.4) is shown in Figure 1 (bold solid line). A strong negative peak at 197 nm is characteristic of irregular structure of peptides and proteins (*39*) and indicates that the peptide main-chain structure of PrP106−126 is disordered. The CD spectrum remained unchanged in several days, demonstrating the stability of the monomeric irregular structure of the peptide in dilute neutral solution. The irregular structure of PrP106−126 is consistent with the NMR observation that the N-terminal half of PrP (including residues 106−126) does not fold into α-helical nor β-sheet structure in aqueous solution (*3*−*7*).

Effects of ganglioside-containing membranes on the secondary structure of PrP106−126 were examined by using liposomes prepared from a 1:1 (w/w) mixture of two brain-extracted lipids, BGS and BPC. BGS is a mixture of various gangliosides, GM1, GD1a, GT1b, etc., in which a polysaccharide head group is linked by a glycosidic bond to a ceramide having two hydrocarbon chains. Due to the presence of sialic acid in the polysaccharide head group, gangliosides have a net negative charge at physiological pH. On the other hand, BPC is a mixture of glycerophospholipids each composed of a neutral (zwitterionic) phosphocholine head group, a glycerol backbone, and two hydrocarbon chain tails. As shown in Figure 1, the CD spectrum of PrP106−126 (25 μM, equivalent to ∼0.05 mg/mL) in the presence of BGS/BPC liposomes exhibits a strong dependence on the lipid concentration. The spectra at relatively low (0−0.3 mg/mL) and high (0.5−2.0 mg/mL) lipid concentrations are drawn with solid and broken lines, respectively, for clarity of presentation.

With an increase of the lipid concentration from 0 to 0.3 mg/mL (solid lines in Figure 1), the negative peak at 197 nm (a marker of irregular structure) becomes smaller and then inverts to a positive one at 196 nm. Concomitantly, a weak and broad negative band grows around 220 nm. The spectrum at the final lipid concentration (0.3 mg/mL, bold solid line) is very close to a typical CD spectrum of a β-sheet structure (*39*). An isodichroic point is seen at 211 nm, indicative of a two-state transition. These CD spectral changes suggest a direct conformational transition from irregular to β-sheet. The conformational transition observed in the low lipid concentration range can be interpreted as follows. At very low lipid concentrations, the membrane can accommodate only a small fraction of the peptide and the peptide molecules densely bound to the membrane adopt a β-sheet structure. The other peptide molecules remain in the solution in an irregular structure. With an increase of the lipid concentration, the population of the membrane-bound peptide increases, and finally at 0.3 mg/mL, almost all the peptide molecules bind to the membrane with a β-sheet structure.

Upon a further increase of the lipid concentration from 0.3 to 2.0 mg/mL (broken lines in Figure 1), the CD spectrum exhibits additional changes different from those observed below 0.3 mg/mL. The strong positive peak at 196 nm characteristic of a β-sheet structure shifts to a shorter wavelength with an isodichroic point at 194 nm. A negative feature with a double minimum at 208 and 218 nm grows significantly. The CD spectrum at the highest lipid concentration (2.0 mg/mL, bold broken line) bears a strong resemblance to that of an α-helix (*39*). These spectral features clearly indicate that the peptide undergoes a direct conformational transition from β-sheet to α-helix with an increase of the lipid concentration. Since all the peptide molecules are expected to be bound to the membrane throughout the high lipid concentration range, the conformational transition from β-sheet to α-helix is attributable to a decrease in the density of the peptide on the membrane. The conversion from a β-sheet conformation to an α-helix conformation of PrP106−126 was also observed when a β-sheet-dominant peptide−liposome mixture was diluted with peptide-free liposomes within a day of sample preparation, suggesting that peptide−peptide and peptide−liposome interactions of β-stranded PrP106−126 may not be so strong as to inhibit individual peptide molecules from migrating on the lipid membrane or from liposome to liposome, at least when the number of molecules involved in the β-sheet is small (see below for the effect of long-term incubation).

To test whether elevation of the peptide density conversely induces an α-helical to β-sheet transition, we have examined

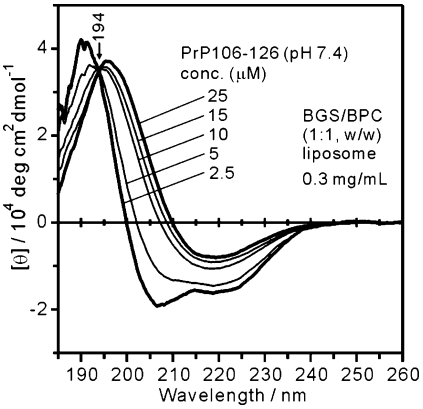

FIGURE 2: Peptide concentration dependence of the CD spectrum of PrP106−126 in the presence of 1:1 (w/w) BGS/BPC liposomes (0.3 mg/mL lipid, pH 7.4). CD spectra were recorded at peptide concentrations of 2.5, 5, 10, 15, and 25 μM as indicated. The spectra mainly due to β-sheet and α-helical structures are emphasized with bold lines. The ordinate shows the molar ellipticity per residue. The arrow indicates an isodichroic point at 194 nm.

the CD spectra at peptide concentrations ranging from 2.5 to 25 μM by successively adding powder of PrP106−126 to a BGS/BPC liposome suspension of 0.3 mg/mL lipid concentration. As Figure 2 shows, the α-helical structure seen at 2.5 μM peptide readily changes to a β-sheet one with an increase of the peptide concentration to 25 μM. The isodichroic point at 194 nm again indicates a direct conversion from α-helical to β-sheet structure. A small difference between the CD spectra of the β-sheet structure (25 mM peptide and 0.3 mg/mL lipid) in Figures 1 and 2 may reflect a small difference in the morphology of the β-sheet structure because the β-sheet structure in Figure 2 was gradually formed by a stepwise peptide addition while that in Figure 1 was formed by mixing the peptide and liposome for a time. The experiments conducted above by varying either the lipid or the peptide concentration clearly show that PrP106−126 takes a β-sheet structure when concentrated on the BGS/BPC membrane at high peptide:lipid ratios, whereas the peptide takes an α-helical structure when diluted at low peptide:lipid ratios. The β-sheet formation at high peptide:lipid ratios is linked with self-association of the peptide.

The secondary structures of PrP106−126 once formed on the BGS/BPC membrane remained stable for at least 3 days when the peptide−liposome mixture was allowed to stand at room temperature. After a week or more, however, tiny precipitates appeared in the peptide−liposome suspension. The precipitation was especially significant for the samples prepared at high peptide:lipid ratios, where significant β-sheet formation was observed. When stained with Congo red, the precipitates exhibited apple-green birefringence under a polarizing microscope (images not shown), indicating that the precipitates were amyloid fibrils (*40*). These observations indicate that the β-sheet structure of PrP106−126 formed on the BGS/BPC membrane can serve as a seed for further polymerization of the peptide into insoluble amyloid fibrils. Such amyloid fibrils were not formed in lipid-free peptide solution even after incubation of several weeks, confirming that the original peptide sample was free of polymerization seeds and the β-sheet formation described above was induced solely by peptide−lipid interactions.

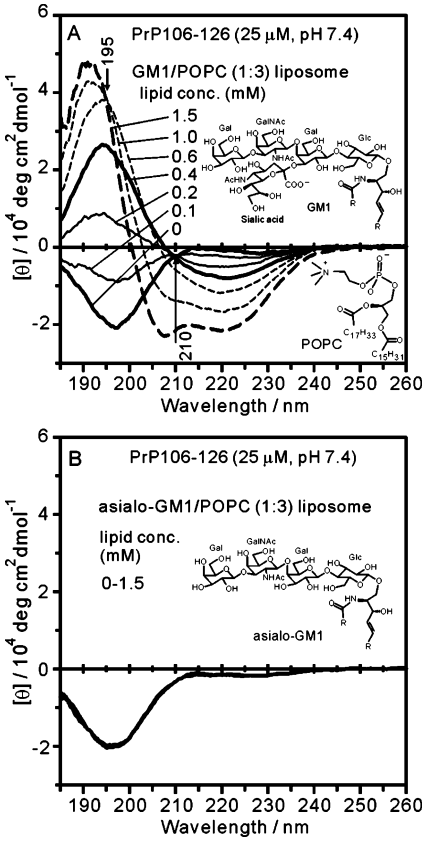

FIGURE 3: CD spectra of PrP106−126 (25 μM, pH 7.4) in the presence of various concentrations of liposomes consisting of a 1:3 (molar ratio) mixture of (A) GM1 and POPC or (B) asialo-GM1 and POPC. In panel A, the spectra at total lipid concentrations of 0, 0.1, 0.2, and 0.4 mM are drawn with solid lines and those at 0.6, 1.0, and 1.5 mM with broken lines. The spectra mainly due to irregular, β-sheet, and α-helical structures are emphasized with bold lines. In panel B, the CD spectrum is independent of the lipid concentration (0−1.5 mM) and all spectra overlap each other.

Ganglioside Negative Charge and Secondary Structure Formation of PrP106−126. To evaluate the possible importance of the ganglioside negative charge in inducing α-helical and β-sheet structures of PrP106−126, we have compared CD spectra of PrP106−126 in the presence of liposomes prepared from two binary mixtures of GM1/POPC and asialo-GM1/POPC. Ganglioside GM1 is a major component of BGS and carries a single sialic acid residue in its head group, whereas asialo-GM1 is identical to GM1 except that it lacks the sialic acid residue and is electrically neutral. POPC is a synthetic neutral (zwitterionic) glycerophospholipid and the main component of BPC. Since only the surface charge differs between the GM1/POPC and asialo-GM1/POPC membranes, these membranes are useful in focusing on the role of the ganglioside negative charge in the secondary structure formation of PrP102−126.

Upon addition of the GM1/POPC membrane (Figure 3A), PrP106−126 exhibits a two-step conformational transition from irregular to β-sheet (lipid concentration range 0−0.4 mM) and from β-sheet to α-helical (0.6−1.5 mM). The two-step transition is very similar to that observed when the BGS/BPC membrane was employed (Figure 1). On the other hand, the asialo-GM1/POPC membrane does not induce any change of the CD spectrum of PrP106−126 (Figure 3B), indicating that the surface negative charge is essential for

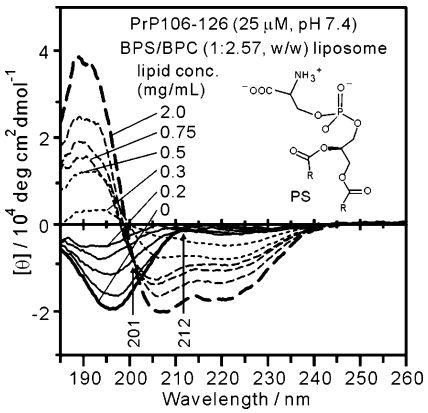

FIGURE 4: CD spectra of PrP106−126 (25 μM, pH 7.4) in the presence of various concentrations of liposomes consisting of a 1:2.57 (w/w) mixture of BPS and BPC. The spectra at total lipid concentrations of 0, 0.025, 0.075, 0.1, 0.2 mg/mL are drawn with solid lines and those at 0.3, 0.5, 0.75, 1.0, 1.5, and 2.0 mg/mL with broken lines. The spectra mainly due to irregular and α-helical structures are emphasized with bold lines. No spectra showed dominance of β-sheet structure. The ordinate shows the molar ellipticity per residue. Isodichroic points at 201 and 212 nm are indicated with arrows.

the binding of PrP102−126 to lipid membranes and for the formation of α-helical and β-sheet structures on the membrane. The importance of electrostatic interactions between the peptide and lipid is supported by the observation that secondary structure formation of PrP106−126 on lipid membranes was significantly delayed by an increase of the ionic strength of the liposome suspension (spectra not shown).

Effect of Negatively Charged Phosphatidylserine. The effect of the membrane negative charge on the secondary structure of PrP106−126 was also examined by using BPS instead of ganglioside BGS. BPS carries one net negative charge on its head group at physiological pH as does the major component GM1 of BGS. BPS-containing liposomes were prepared from a 1:2.57 (w/w) BPS/BPC mixture, the mixing ratio being adjusted to produce the same overall density of negative charge (the amount of negative charge per unit mass of the lipid) as the 1:1 (w/w) BGS/BPC mixture used above.

Figure 4 shows CD spectra of PrP106−126 (25 μM) mixed with varied amounts of the BPS/BPC membrane. With an increase of the lipid concentration from 0 to 0.2 mg/mL, the negative peak at 196 nm characteristic of irregular structure diminishes and a weak broad feature appears around 220 nm. The isodichroic point at 212 nm is analogous to that observed at 211 nm during the irregular to β-sheet transition in the presence of the BGS/BPC membrane (Figure 1). Thus, the CD spectral change in this lipid concentration range suggests a partial structural transition from irregular to β-sheet. A further increase of the lipid concentration, however, does not produce a spectrum attributable to a β-sheet-dominant state. Rather, the CD spectrum changes toward an α-helical one with an isodichroic point at 201 nm in the 0.5−2.0 mg/mL range, implying an equilibrium between membrane-bound α-helical and nonbound irregular structures. The spectrum at the highest lipid concentration (2.0 mg/mL) is close to that observed when the peptide was highly diluted with BGS/BPC membranes (Figure 1), suggesting that PrP106−126 binds to the BPS/BPC and BGS/BPC membranes in a common manner at low peptide:lipid ratios. At high peptide:lipid ratios (or at low lipid concentrations), however, the phosphatidylserine-containing membrane (BPS/BPC) is much less effective than the ganglioside-containing membrane (BGS/BPC) in inducing the β-sheet structure of PrP106−126. Since the overall negative charge density is equivalent between the BGS/BPC and BPS/BPC membranes, the difference in β-sheet-inducing ability may be ascribed to a difference in the negative charge distribution on the membrane surface, reflecting the structural difference between ganglioside and phosphatidylserine.

Relationship between Lateral Phase Separation and β-Sheet Formation. Ganglioside differs from a glycerophospholipid such as phosphatidylserine in two major structural aspects besides the head group structure. The region linking the polar head group and the hydrophobic tail of ganglioside contains both proton donors (NH and OH) and acceptors (C═O, esteric O, and OH), whereas the corresponding linker region of glycerophospholipid contains only proton acceptors (C═O and esteric O) (*41*, *42*). Accordingly, ganglioside molecules can form hydrogen bonds with each other in both the linker and the polar head group regions, whereas glycerophospholipids are capable of hydrogen bonding in the head group region only. Another difference between ganglioside and glycerophospholipid lies in the structure of the hydrophobic tails. In most naturally occurring glycerophospholipids, the acyl chain bound to carbon *sn*-2 of glycerol is kinked at a single or multiple *cis* C═C bond(s), whereas most gangliosides have only one *trans* C═C bond, allowing extension of their hydrocarbon chains without kink (*43*, *44*). Since unkinked hydrocarbon chains can be packed more tightly than those having kinks, mutual attraction of the tail region is also stronger in ganglioside than in glycerophospholipid. As a consequence of these structural differences, ganglioside tends to self-aggregate laterally in the membrane when mixed with glycerophospholipids (*32*−*36*). The strong β-sheet-inducing ability of ganglioside-containing membranes (BGS/BPC and GM1/POPC) may be associated with lateral phase separation that produces clusters of negatively charged ganglioside molecules.

Lateral phase separation is not limited to ganglioside-containing membranes but also occurs in mixtures of two glycerophospholipids with significantly different melting temperatures (T_m) (*45*, *46*). In the temperature range between the T_m values of two lipid components, the lipid molecules with the higher T_m tend to gather with each other to form gel domains, whereas the lipid with the lower T_m melts into a fluid and surrounds the gel domains (*47*). This is because intermolecular interaction is stronger among lipid molecules with the higher T_m than with the lower T_m, and the lipid molecules with the higher T_m tend to gather with each other.

To investigate the effect of negative charge clusters on the secondary structure formation of PrP106−126, we have prepared liposomes from binary mixtures of negatively charged glycerophospholipid DMPS or POPS and neutral glycerophospholipid POPC. DMPS has a negatively charged phosphoserine head group and two saturated myristoyl (C14:0) tails with a T_m of 36 °C (*48*). On the other hand, POPC has a neutral (zwitterionic) phosphocholine head group and a pair of saturated palmitoyl (C16:0) and unsaturated oleoyl (C18:1) tails. Owing to the presence of a *cis* C═C bond in the oleoyl tail, the T_m of POPC is low (−2 °C) (*49*). Since

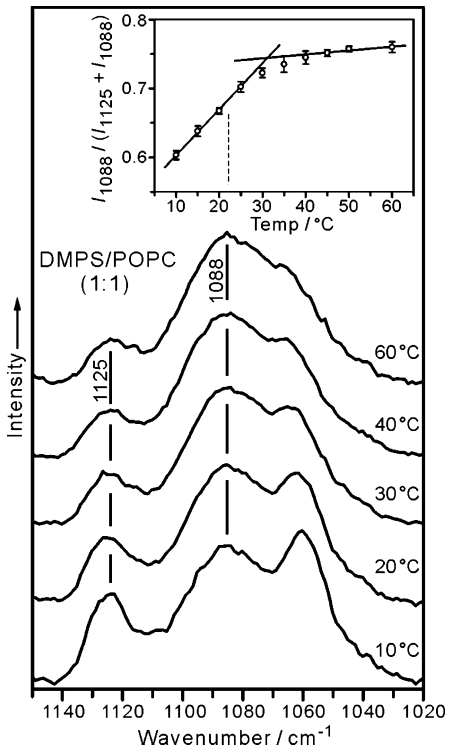

FIGURE 5: Raman spectra of liposomes prepared from an equimolar mixture of DMPS and POPC (2.5 mM each, pH 7.4) at 10, 20, 30, 40, and 60 °C from bottom to top. The inset shows a plot of the peak intensity ratio, $I_{1088}/(I_{1125} + I_{1088})$, against temperature. The intensity ratio serves as a measure of the *gauche* content in the lipid hydrocarbon chains. Straight lines show the slopes of the intensity change, and the temperature at their intersection (~32 °C) indicates the phase transition temperature, which is much higher than room temperature (~22 °C).

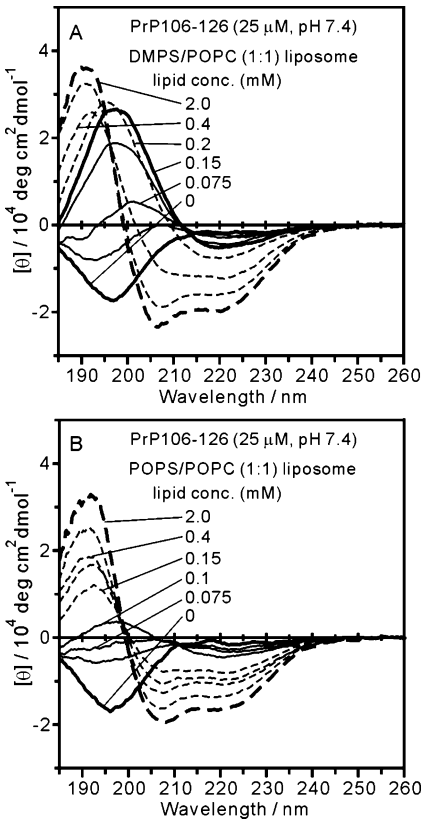

FIGURE 6: CD spectra of PrP106−126 (25 μM, pH 7.4) in the presence of various concentrations of (A) DMPS/POPC and (B) POPS/POPC liposomes. The molar ratio of two lipid components was 1:1 for both mixtures. In panel A, the spectra at total lipid concentrations of 0, 0.05, 0.075, 0.1, and 0.15 mM are drawn with solid lines and those at 0.2, 0.4, 1.0, and 2.0 mM with broken lines. The spectra mainly due to irregular, β-sheet, and α-helical structures are emphasized with bold lines. In panel B, the spectra at total lipid concentrations of 0, 0.05, 0.075, and 0.1 mM are drawn with solid lines and those at 0.15, 0.2, 0.4, 1.0, and 2.0 mM with broken lines. The spectra mainly due to irregular and α-helical structures are emphasized with bold lines. No spectra showed dominance of β-sheet structure in the presence of POPS/POPC liposomes.

the T_m values of DMPS and POPC are much higher and lower than room temperature, respectively, binary mixtures of DMPS and POPC are expected to show lateral phase separation at room temperature. On the other hand, if we replace DMPS with POPS, which differs from POPC only in having a negative charge in the head group and a somewhat higher T_m of 14 °C (*50*), no lateral phase separation is expected at room temperature because the T_m is much lower than room temperature for both lipid components POPS and POPC.

Lateral phase separation can be detected by Raman spectroscopy. With an increase of the temperature, the gel domain composed of the lipid component with the higher T_m gradually melts into a fluid and the melting is accompanied by conformational transition from *trans* to *gauche* about C−C bonds of the lipid hydrocarbon chains. Such conformational transition manifests itself in the Raman spectrum as a change in the relative intensity of the Raman bands due to *trans* and *gauche* conformers (*51*). Figure 5 shows Raman spectra of the 1:1 DMPS/POPS liposome at varied temperatures in the 1150−1020 cm^{-1} C−C stretching region. The Raman band at 1125 cm^{-1} is exclusively assigned to *all-trans* conformers, whereas the broad feature peaking at 1088 cm^{-1} is contributed by *gauche* conformers and less significantly by *trans* conformers (*52*). The phosphocholine head groups also contribute to the 1088 cm^{-1} feature to some extent (*52*). Although the 1088 cm^{-1} band is not a pure *gauche* band, the peak height ratio of the 1125 and 1088 cm^{-1} bands is known to provide a convenient means for monitoring the melting of lipid membranes (*52*). Here we employed the ratio of the 1088 cm^{-1} peak height (I_{1088}) to the sum of the 1125 and 1088 cm^{-1} peak heights ($I_{1125} + I_{1088}$) as a measure of the *gauche* content. The intensity ratio $I_{1088}/(I_{1125} + I_{1088})$ is plotted against the temperature in the inset of Figure 5. The ratio linearly increases with temperature below 30 °C, whereas it stays almost constant above 30 °C. Such an abrupt change of the slope is caused by completion of melting of the higher T_m lipid component, and the intersection point of the two slope lines is regarded as indicating the transition from the gel + fluid phase to the fluid-only phase (*47*). The transition temperature estimated from the intersection point (32 °C) is much higher than room temperature (~22 °C) as expected. Therefore, the Raman spectra in Figure 5 confirm that lateral phase separation really occurs in the 1:1 DMPS/POPS membrane at room temperature. On the other hand, Raman spectra of the 1:1 POPS/POPC membrane did not show a significant change above room temperature (data not shown), confirming that both lipid components are in the fluid state and are fully mixed with each other at room temperature.

Figure 6A shows CD spectra of PrP106−126 mixed with a varied amount of the 1:1 DMPS/POPC membrane at room

temperature. The CD spectrum at 0.15 mM lipid concentration is very close to that of a β-sheet structure found in the presence of the BGS/BPC membrane (Figure 1), indicating that the DMPS/POPC membrane is as effective as the BGS/BPC membrane in inducing a β-sheet structure of PrP106−126. In contrast, no β-sheet-dominant state is reached by the peptide when mixed with the 1:1 POPS/POPC membrane (Figure 6B). As shown by Raman spectroscopy, negatively charged DMPS molecules are clustered in the 1:1 DMPS/POPC membrane at room temperature because of lateral phase separation, whereas no clustering of POPS molecules occurs in the 1:1 POPS/POPC membrane. Therefore, it is concluded that clustered negative charges on the lipid membrane surface are particularly effective in inducing the β-sheet formation of PrP106−126.

DISCUSSION

Interaction between the Membrane Negative Charge and PrP106−126. The peptide fragment corresponding to residues 106−126 of PrP is known to be amyloidogenic and to exhibit a strong tendency to aggregate into a β-sheet structure under certain solution conditions of concentration, pH, and ionic strength (*28*−*30*). In this study, we have examined the role of negatively charged lipid membranes in the β-sheet formation of PrP106−126 by using the solution conditions that do not induce spontaneous aggregation of the peptide, namely, 25 mM peptide, pH 7.4, and minimal ionic strength. We paid special attention to avoid unnecessary aggregation of the peptide in all aspects of sample manipulation. The stability and reproducibility of the CD spectra reported here confirm that no spontaneous aggregation occurred throughout the experiment. The secondary structure formation of PrP106−126 reported in this study is thus associated with the peptide−lipid interactions.

One of our novel findings is that PrP106−126 binds to negatively charged lipid membranes but not to neutral membranes. This observation indicates that electrostatic interaction plays a key role in the membrane binding of PrP106−126. PrP106−126 contains two positively charged amino acid residues, Lys106 and Lys110, and their side-chain amino groups are expected to interact with negatively charged lipid head groups on the membrane. CD spectra have shown that the peptide binds to the membrane in an α-helical structure at low peptide:lipid ratios (e.g., see Figure 1). Since amino acid side chains stick out with a pitch of 3.6 residues per turn in an α-helix, the side chains of Lys106 and Lys110 separated by three intervening residues are expected to be located on the same side of the α-helix, facilitating the interaction with the negatively charged membrane surface. The α-helical structure found at low peptide:lipid ratios may be most suitable for single molecular interaction of PrP106−126 with negatively charged membranes. Liposomes bound by α-helical PrP106−126 were stable for days as described in the Results, indicating that the interaction between α-helical PrP106−126 and the lipid membrane is not so strong as to destabilize the liposome structure.

At high peptide:lipid ratios, where the peptide molecules were expected to be associated with each other, negatively charged lipid membranes induced the β-sheet formation of PrP106−126, especially when the negative charges were clustered on the membrane surface (e.g., see Figure 1). Generally, β-sheet structures are stabilized by hydrogen bonding among the main-chain amide groups of adjacent β-strands, and the side chains of each β-strand stick out on alternative sides of the plane of amide hydrogen bonding. Thus, the side chains of Lys106 and Lys110 of PrP106−126 are expected to be located on the same side of the peptide backbone in a β-strand, allowing interaction of the cationic amino groups of both Lys side chains with negatively charged sites on the membrane. Although the electrostatic interaction of a β-strand of PrP106−126 with negatively charged membranes may not be so strong as to transform the structure of a single PrP106−126 molecule from α-helix to β-sheet, interstrand main-chain hydrogen bonding and cooperative Lys−membrane attraction involving multiple β-strands of a β-sheet would be strong enough to stabilize self-associated β-strands compared to dispersed α-helices. This may be the reason why PrP106−126 takes a β-sheet structure when concentrated on negatively charged membranes.

Complete or almost complete β-sheet formation was observed in the presence of BGS/BPC (Figures 1 and 2), GM1/POPC (Figure 3), and DMPS/POPC (Figure 6) membranes. The BGS/BPC and GM1/POPC membranes are binary mixtures of ganglioside and phosphatidylcholine, in which lateral phase separation has been shown to occur by using differential scanning calorimetry (*32*, *33*), freeze-etch electron microscopy (*34*), and atomic force microscopy (*35*, *36*). For the DMPS/POPC membrane system, the present Raman spectroscopic analysis has demonstrated the occurrence of lateral phase separation (Figure 5). Since negatively charged ganglioside and DMPS molecules form clusters in the membrane due to lateral phase separation, clustering of negatively charged lipid head groups on the membrane surface is concluded to be essential for the efficient β-sheet formation of PrP106−126. The importance of clustered negative charges in the β-sheet formation is consistent with the observation that neither the neutral asialo-GM1/POPC membrane (Figure 3B) nor membranes with nonclustered negative charges (BPS/BPC in Figure 4 and POPS/POPC in Figure 6B) induced significant β-sheet formation.

The state of negative charge distribution, clustered or nonclustered, seems to also affect the affinity of PrP106−126 to the lipid membrane. In the presence of clustered membrane negative charges, the peptide showed a two-step conformational transition from irregular to β-sheet and β-sheet to α-helix as evidenced by two isodichroic points around 210 and 195 nm, respectively, in the CD spectra (Figures 1, 3A, and 6A). This observation clearly indicates that all the peptide molecules must be bound to the membrane in either β-sheet or α-helical structure at low peptide:lipid ratios (at high lipid concentrations) where the membrane provides sufficient peptide binding sites. In the presence of nonclustered negative charges, on the other hand, only one isodichroic point was observed around 200 nm at low peptide:lipid ratios (Figures 4 and 6B). The isodichroic point is attributable to a conformational transition from irregular to α-helix and suggests that some peptide molecules may be unbound from the membrane with an irregular structure even if there are enough peptide binding sites. Therefore, it is likely that PrP106−126 exhibits higher affinity for clustered negative charges than for nonclustered negative charges.

The mechanism of β-sheet formation of PrP102−126 on the membranes containing clustered negative charges may be as follows. The negative charge clusters attract PrP106−126 molecules through interaction with the positively charged Lys side chains. Such an increase of the local density of the peptide increases the chance of peptide self-association. The self-associated peptide molecules form a β-sheet because of the stabilization by intermolecular main-chain hydrogen bonding and by cooperative electrostatic interaction of the cationic Lys side chains with negative charge clusters on the membrane surface. The β-sheet thus formed serves as a seed for further polymerization of the peptide into fibrils.

Pathological Significance of β-Sheet Formation of PrP106−126 on the Membrane Surface. Several lines of evidence have shown that there are at least two modes of interaction between PrP^C and the plasma membrane besides the insertion of a GPI anchor. One interaction mode involves the N-terminal region of PrP^C (N-terminus to residue 90). The N-terminal region is necessary for the binding of PrP^C to detergent-resistant cellular membranes (*53*) or to artificial membranes containing phosphatidylcholine, sphingomyelin, cerebroside, and cholesterol, but not ganglioside (*54*). The latter membrane system bears no net charge at physiological pH, indicating that the N-terminal membrane binding does not involve electrostatic interactions between the protein and the membrane surface.

Another membrane binding mode is seen for the C-terminus to residue 90 and is considered to be at least partly governed by electrostatic interactions. For example, recombinant Syrian hamster PrP90−231, which lacks the N-terminal membrane binding region and comprises the protease-resistant portion of PrP^{Sc} (*11*), is capable of binding to negatively charged glycerophospholipid membranes with a concomitant partial conformational transition from α-helix to β-sheet (*23*). This observation suggests that the C-terminal charge-dependent membrane binding mode plays a role in the conversion from PrP^C to PrP^{Sc}. A PrP segment spanning residues 106−126, which corresponds to the peptide PrP106−126 studied here, is included in the C-terminal membrane binding region. In this study, we have demonstrated that PrP106−126 can form a self-associated β-sheet upon interaction with clustered negative charges on the lipid membrane surface. Both PrP^C and PrP^{Sc} are colocalized in caveolae of neuroblastoma cells (*12*, *13*), and caveolae are enriched with negatively charged ganglioside (*15*, *16*). In addition, clusters of negative charges are formed in ganglioside-containing membranes due to lateral phase separation (*31*−*36*). Therefore, it is possible that PrP^C changes into β-sheet-rich pathogenic PrP^{Sc} through interaction of the residue 106−126 region with negative charges of clustered ganglioside molecules in caveolae. Such conformational conversion would be particularly significant when PrP^C is abnormally concentrated in caveolae or template PrP^{Sc} (endogenous or exogenous) is already present in caveolae.

REFERENCES

1. Stahl, N., Borchelt, D. R., Hsiao, K., and Prusiner, S. B. (1987) Scrapie prion protein contains a phosphatidylinositol glycolipid, *Cell 51*, 229−240.
2. Liao, Y. C., Lebo, R. V., Clawson, G. A., and Smuckler, E. A. (1986) Human prion protein cDNA: molecular cloning, chromosomal mapping, and biological implications, *Science 233*, 364−367.
3. Donne, D. G., Viles, J. H., Groth, D., Mehlhorn, I., James, T. L., Cohen, F. E., Prusiner, S. B., Wright, P. E., and Dyson, H. J. (1997) Structure of the recombinant full-length hamster prion protein PrP(29−231): The N terminus is highly flexible, *Proc. Natl. Acad. Sci. U.S.A. 94*, 13452−13457.
4. Riek, R., Hornemann, S., Wider, G., Glockshuber, R., and Wuthrich, K. (1997) NMR characterization of the full-length recombinant murine prion protein, mPrP(23−231), *FEBS Lett. 413*, 282−288.
5. Wright, P., and Dyson, H. J. (1997) Structure of the recombinant full-length prion protein PrP(29−231): The N-terminus is highly flexible, *Proc. Natl. Acad. Sci. U.S.A. 94*, 13452−13457.
6. Zahn, R., Liu, A., Luhrs, T., Riek, R., von Schroetter, C., Lopez Garcia, F., Billeter, M., Calzolai, L., Wider, G., and Wuthrich, K. (2000) NMR solution structure of the human prion protein, *Proc. Natl. Acad. Sci. U.S.A. 97*, 145−150.
7. Lopez-Garcia, F., Zahn, R., Riek, R., and Wutrich, K. (2000) NMR structure of the bovine prion protein, *Proc. Natl. Acad. Sci. U.S.A. 97*, 8334−8339.
8. Pan, K., Baldwin, M., Nguyen, J., Gasset, M., Serban, A., Groth, D., Mehlhorn, I., Huang, Z., Fletterick, R. J., Cohen, F. E., and Prusiner, S. B. (1993) Conversion of α-helices into β-sheets features in the formation of the scrapie prion proteins, *Proc. Nat. Acad. Sci. U.S.A. 90*, 10962−10966.
9. Prusiner, S. B. (1991) Molecular biology of prion diseases, *Science 252*, 1515−1522.
10. Prusiner, S. B. (1997) Prion diseases and the BSE crisis, *Science 278*, 245−251.
11. Prusiner, S. B. (1998) Prions, *Proc. Natl. Acad. Sci. U.S.A. 95*, 13363−13383.
12. Vey, M., Pilkuhn, S., Wille, H., Nixon, R., DeArmond, S. J., Smart, E. J., Anderson, R. W. G., Taraboulos, A., and Prusiner, S. B. (1996) Subcellular colocalization of the cellular and scrapie prion proteins in caveolae-like membranous domains, *Proc. Natl. Acad. Sci. U.S.A. 93*, 14945−14949.
13. Naslavsky, N., Stein, R., Yanai, A., Friedlander, G., and Taraboulos, A. (1997) Characterization of detergent-insoluble complexes containing the cellular prion protein and its scrapie isoform, *J. Biol. Chem. 272*, 6324−6331.
14. Okamoto, T., Schlegel, A., Scherer, P. E., and Lisanti, M. P. (1998) Caveolins, a family of scaffolding proteins for organizing "pre-assembled signaling complexes" at the plasma membrane, *J. Biol. Chem. 273*, 5419−5422.
15. Parton, R. G. (2003) Caveolae—from ultrastructure to molecular mechanisms, *Nat. Rev. Mol. Cell Biol. 4*, 162−167.
16. Parton, R. G. (1994) Ultrastructural localization of gangliosides: GM1 is concentrated in caveolae, *J. Histochem. Cytochem. 42*, 155−166.
17. Hooper, N. M. (1999) Detergent-insoluble glycosphingolipid/cholesterol-rich membrane domains, lipid rafts and caveolae, *Mol. Membr. Biol. 16*, 145−156.
18. Mayor, S., Rothberg, K. G., and Maxfield, F. R. (1994) Sequestration of GPI-anchored proteins in caveolae triggered by cross-linking, *Science 264*, 1948−1951.
19. Taraboulos, A., Scott, M., Semenov, A., Avraham, D., Laszlo, L., and Prusiner, S. B. (1995) Cholesterol depletion and modification of COOH-terminal targeting sequence of the prion inhibit formation of scrapie isoform, *J. Cell Biol. 129*, 121−132.
20. Bate, C., Salmona, M., Diomede, L., and Williams, A. (2004) Squalestatin cures prion-infected neurons and protects against prion neurotoxicity, *J. Biol. Chem. 279*, 14983−14990.
21. Kaneko, K., Vey, M., Scott, M., Pilkuhn, S., Cohen, F. E., and Prusiner, S. B. (1997) COOH-terminal sequence of the cellular prion protein directs subcellular trafficking and controls conversion into the scrapie isoform, *Proc. Natl. Acad. Sci. U.S.A. 94*, 2333−2338.
22. Morillas, M., Swietnicki, W., Gambetti, P., and Surewicz, W. K. (1999) Membrane environment alters the conformational structure of the recombinant human prion protein, *J. Biol. Chem. 274*, 36859−36865.
23. Sanghera, N., and Pinheiro, T. J. T. (2002) Binding of prion protein to lipid membranes and implications for prion conversion, *J. Mol. Biol. 315*, 1241−1256.
24. Critchley, P., Kazlauskaite, J., Eason, R., and Pinheiro, T. J. T. (2004) Binding of prion proteins to lipid membranes, *Biochem. Biophys. Res. Commun. 313*, 559−567.
25. Mattei, V., Garofalo, T., Misasi, R., Gizzi, C., Mascellino, M. T., Dolo, V., Pontieri, G. M., Sorice, M., and Pavan, A. (2002) Association of cellular prion protein with gangliosides in plasma

membrane microdomains of neural and lymphocytic cells, *Neurochem. Res. 27*, 743−749.
26. Forloni, G., Angeretti, N., Chiesa, R., Monzani, E., Salmona, M., Bugiani, O., and Tagliavini, F. (1993) Neurotoxicity of a prion protein fragment, *Nature 362*, 543−546.
27. Deli, M. A., Sakaguchi, S., Nakaoke, R., Ábrahám, C. S., Takahata, H., Kopaĉek, J., Shigematsu, K., Katamine, S., and Niwa, M. (2000) PrP fragment 106−126 is toxic to cerebral endothelial cells expressing PrPC, *Neuroreport 11*, 3931−3936.
28. Selvaggini, C., De Gioia, L., Cantù, L., Ghibaudi, E., Diomede, L., Passerini, F., Forloni, G., Bugiani, O., Tagliavini, F., and Salmona, M. (1993) Molecular characteristics of a protease-resistant, amyloidogenic and neurotoxic peptide homologous to residues 106−126 of the prion protein, *Biochem. Biophys. Res. Commun. 194*, 1380−1386.
29. De Gioia, L., Selvaggini, C., Ghibaudi, E., Diomede, L., Bugiani, O., Forloni, G., Tagliavini, F., and Salmona, M. (1994) Conformational polymorphism of the amyloidogenic and neurotoxic peptide homologous to residues 106−126 of the prion protein, *J. Biol. Chem. 269*, 7859−7862.
30. Rymer, D. L., and Good, T. A. (2000) The role of prion peptide structure and aggregation in toxicity and membrane binding, *J. Neurochem. 75*, 2536−2545.
31. Sharom, F. J., and Grant, C. W. (1977) A ganglioside spin label: ganglioside head group interactions, *Biochem. Biophys. Res. Commun. 74*, 1039−1045.
32. Masserini, M., and Freire, E. (1986) Thermotropic characterization of phosphatidylcholine vesicles containing ganglioside GM1 with homogeneous ceramide chain length, *Biochemistry 25*, 1043−1049.
33. Tillack, T. W., Wong, M., Allietta, M., and Thompson, T. E. (1982) Organization of the glycosphingolipid asialo-GM1 in phosphatidylcholine bilayers, *Biochim. Biophys. Acta 691*, 261−273.
34. Terzaghi, A., Tettamanti, G., and Masserini, M. (1993) Interaction of glycosphingolipids and glycoproteins: thermotropic properties of model membranes containing GM1 ganglioside and glycophorin, *Biochemistry 32*, 9722−9725.
35. Vié, V., Van Mau, N., Lesniewska, E., Goudonnet, J. P., Heitz, F., and Le Grimellec, C. (1998) Distribution of ganglioside GM1 between two-components, two-phase phosphatidylcholine monolayers, *Langmuir 14*, 4574−4583.
36. Ohta, Y., Yokoyama, S., Sakai, H., and Abe, M. (2004) Membrane properties of binary and ternary systems of ganglioside GM1/dipalmitoylphosphatidylcholine/dioleoylphosphatidyl-choline, *Colloids Surf., B 34*, 147−153.
37. Svennerholm, L. (1963) Chromatographic separation of human brain gangliosides, *J. Neurochem. 10*, 613−623.
38. MacDonald, R. C., MacDonald, R. I., Menco, B. P., Takeshita, K., Subbarao, N. K., and Hu, L. R. (1991) Small-volume extrusion apparatus for preparation of large, unilamellar vesicles, *Biochim. Biophys. Acta 1061*, 297−303.
39. Brahms, S., and Brahms, J. (1980) Determination of protein secondary structure in solution by vacuum ultraviolet circular dichroism, *J. Mol. Biol. 138*, 149−178.
40. Wolman, M., and Bubis, J. J. (1965) The cause of the green polarization color of amyloid stained with Congo red, *Histochemie 4*, 351−356.
41. Pascher, I. (1976) Molecular arrangements in sphingolipids. Conformation and hydrogen bonding of ceramide and their implication on membrane stability and permeability, *Biochim. Biophys. Acta 455*, 433−451.
42. Boggs, J. M. (1987) Lipid intermolecular hydrogen bonding: influence on structural organization and membrane function, *Biochim. Biophys. Acta 906*, 353−404.
43. Degroote, S., Wolthoorn, J., and van Meer, G. (2004) The cell biology of glycosphingolipids, *Semin. Cell Dev. Biol. 15*, 375−387.
44. Karlsson, K.-A. (1970) Sphingolipid long chain bases, *Lipids 5*, 878−891.
45. Shimshick, E. J., and McConnell, M. (1973) Lateral phase separation in phospholipid membranes, *Biochemistry 12*, 2351−2360.
46. Lee, A. G. (1977) Lipid phase transitions and phase diagrams. II. Mixtures involving lipids, *Biochim. Biophys. Acta 472*, 285−344.
47. Luna, E. J., and McConnell, H. M. (1977) Lateral phase separations in binary mixtures of phospholipids having different charges and different crystalline structures, *Biochim. Biophys. Acta 470*, 303−316.
48. Browning, J. L., and Seelig, J. (1980) Bilayers of phosphatidylserine: a deuterium and phosphorus nuclear magnetic resonance study, *Biochemistry 19*, 1262−1270.
49. Lavialle, F., and Levin, I. W. (1980) Raman spectroscopic study of the interactions of dimyristoyl- and 1-palmitoyl-2-oleoylphosphatidylcholine liposomes with myelin proteolipid apoprotein, *Biochemistry 19*, 6044−6050.
50. Mattai, J., Hauser, H., Demel, R. A., and Shipley, G. G. (1989) Interactions of metal ions with phosphatidylserine bilayer membranes: effect of hydrocarbon chain unsaturation, *Biochemistry 28*, 2322−2330.
51. Lippert, J. L., and Peticolas, W. L. (1971) Laser Raman investigation of the effect of cholesterol on conformational changes in dipalmitoyl lecithin multilayers, *Proc. Natl. Acad. Sci. U.S.A. 68*, 1572−1576.
52. Levin, I. W. (1984) Vibrational spectroscopy of membrane assemblies, in *Advances in Infrared and Raman Spectroscopy* (Clark, R. J. H., and Hester, R. E., Eds.) Vol. 11, pp 1−48, John Wiley & Sons, New York.
53. Walmsley, A. R., Zeng, F., and Hooper, N. M. (2003) The N-terminal region of the prion protein ectodomain contains a lipid raft targeting determinant, *J. Biol. Chem. 278*, 37241−37248.
54. Baron, G. S., and Caughey, B. (2003) Effect of glycosylphosphatidylinositol anchor-dependent and -independent prion protein association with model raft membranes on conversion to the protease-resistant isoform, *J. Biol. Chem. 278*, 14883−14892.

BI700939J